

Analysis of JT-60SA scenarios on the basis of JET and JT-60U discharges

J. Garcia¹, N. Hayashi², G. Giruzzi¹, M. Schneider¹, E. Joffrin¹, S. Ide², Y. Sakamoto², T. Suzuki², H. Urano², the JT-60U Team and the JET EFDA contributors*

JET-EFDA, Culham Science Centre, Abingdon, OX14 3DB, UK

¹CEA, IRFM, 13108 Saint-Paul-lez-Durance, France

²Japan Atomic Energy Agency, Mukouyama, Naka City, Ibaraki, 311-0193 Japan
e-mail: jeronimo.garcia@cea.fr

Introduction

Validation of the main models available for the plasma simulation is mandatory. These include, e.g., energy and particle transport, current, rotation and their sources, pedestal pressure and fast particles. JT-60SA [1] is a machine designed on the basis of the results of JT-60U, and using an upgrade of the JT-60U Neutral Beam Injection (NBI) system; on the other hand, it has practically the same size as JET, which also has NBI as the main heating and current drive system. Therefore, it appears that simulations of JT-60SA scenarios should be based at least on experimental results of the two machines that are the most similar, for size and configuration: JT-60U and JET. For this purpose, in the framework of a broad research plan based on JT-60SA [1], a series of representative discharges of the three main operational scenarios, H-mode, hybrid and steady-state, have been selected for each device. A subset of these discharges, inductive H-modes and hybrids are discussed in this paper. The selected time for the analysis concentrates on the phase of highest performance of each of these discharges.

Predictive simulations for the temperature profiles have been carried out with three transport models, Bohm-GyroBohm (BGB) [2], CDBM [3] and GLF23 [4], and by adjusting, as a first step, the pedestal, rotation and density to experimental values whenever available. To carry out this programme, the integrated modelling codes CRONOS [5] and TOPICS [6] have been used in order to benchmark the models in both codes. Later, predictive particle transport simulations have been performed with GLF23. Finally, fully predictive simulations of temperatures, density and pedestal have been performed. The pedestal temperature is calculated by using the so-called Cordey two-term scaling [7]. With this approach, calculations for JT-60SA have been carried out.

Analysis of JET and JT-60U discharges. Extrapolation to JT-60SA

Heat transport has been analysed in two discharges from JT-60U, inductive H-mode #33655 and Hybrid #48158, and two discharges from JET, inductive H-mode #73344 and hybrid #75225, with CRONOS and TOPICS by using three different transport models, GLF23, BGB and CDBM. The density and q profiles for both discharges are kept fixed during the simulation and just the temperatures are predicted. The NBI power is calculated by means of the code OFMC for the JT-60U discharges and NEMO/SPOT for the JET ones. In figure 1, the results for the inductive H-modes #33655 and #73344 are compared to the experimental data, showing a good agreement between both codes and with experimental data. On the other hand, for the hybrid shots #48158 and #75225, shown in figure 2, although both codes give similar results, they deviate more from experimental data, mainly for ions, for which a too

* See the Appendix of F. Romanelli et al., Proceedings of the 24th IAEA Fusion Energy Conference 2012, San Diego, USA

high temperature is obtained with the models GLF23 and BGB whereas CDBM tends to be closer.

Particle transport has been analysed by using the CRONOS code and the GLF23 transport model. Density at the top of the pedestal has been fixed to experimental value. Two different configurations have been applied depending of the type of scenario. For the inductive H-mode discharges only GLF23 has been used for both heat and particle transport whereas for hybrids, GLF23 or CDBM have been applied for heat transport and GLF23 for particle transport. In figure 3 results are compared with experimental data. Density profiles are well simulated and in particular GLF23 is able to reproduce the increase of density peaking usually obtained in advanced regimes. For these regimes, the use of different transport models for heat transport give a margin of confidence.

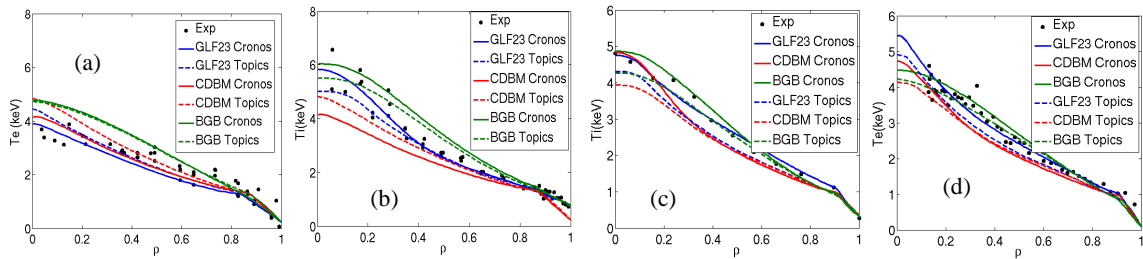


Figure 1 Comparison between the electron and ion temperatures profiles with those obtained with CRONOS and TOPICS with GLF23, CDBM and Bohm-GyroBohm transport models for the JT-60U shot 33655 at $t=8.0s$ (a,b) and JET shot 73344 at $t=19.5s$ (c,d)

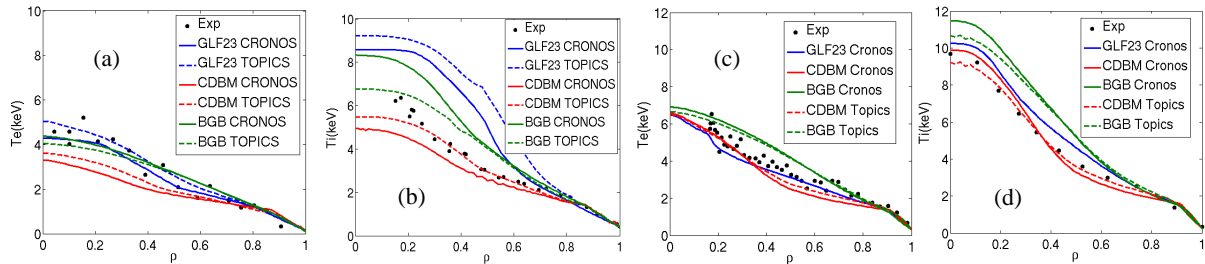


Figure 2 Comparison between the electron and ion temperatures profiles with those obtained with CRONOS and TOPICS with GLF23, CDBM and Bohm-GyroBohm transport models for the JT-60U shot 48158 at $t=27.0s$ (a,b) and JET shot 75225 at $t=6.02s$ (c,d)

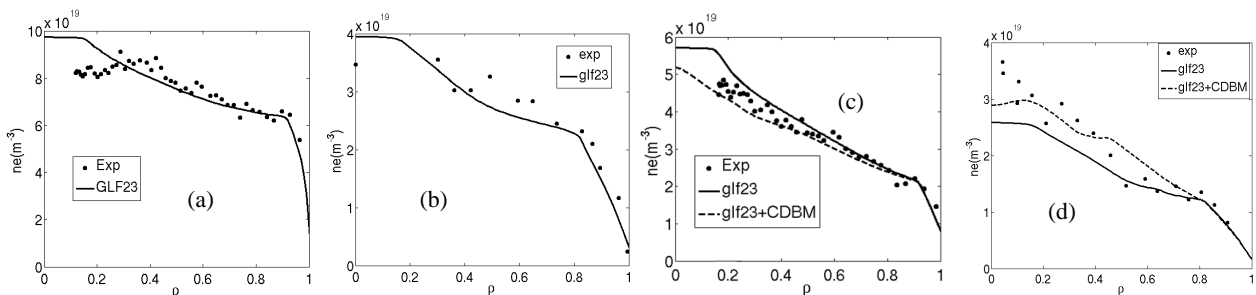


Figure 3 Comparison between the electron density profiles, with those obtained with CRONOS and GLF23. GLF23 or CDBM have been used for the heat transport. JET discharges #73344(a) and #75225(c), JT-60U discharges #33655 (b) and #48158(d)

Fully predictive simulations including heat and particle transport, heat sources, current diffusion and pedestal pressure have been performed with the CRONOS code. In order to quantify the global accuracy of the set of different simulations and models applied, a statistical analysis has been carried out. For this purpose the standard expression for the root-mean-square (rms) deviation

$$rms = \left[\frac{1}{N} \sum_{i=1}^N \frac{\{X_{exp,i} - X_{sim,i}\}^2}{X_{exp,i}^2} \right]^{1/2} \quad (1)$$

has been used, where $X_{exp,i}$ is the value obtained from experimental profiles and $X_{sim,i}$ the simulated one for each of the predictions performed in this section, whereas N is the total number of simulations. The global variables selected for the comparison and the rms obtained for each one are shown in table I. The calculation shows that the results are reasonably close to the experimental data. The maximum rms obtained is below 20% and it corresponds to the pedestal pressure, 18.2%.

Discharge	β_N	$H_{98}(y,2)$	f_{Gr}	$\langle ne \rangle 10^{19} \text{ m}^{-3}$	$\langle Te \rangle \text{ keV}$	$\langle Ti \rangle \text{ keV}$	$P_{ped}(\text{kPa})$
Inductive H-mode 33654	1.1/1.3	0.65/0.85	0.42/0.48	2.3/2.4	2.0/2.7	3.2/3.4	13/15
Inductive H-mode 73344	1.7/1.5	0.97/0.85	0.80/0.75	6.75/6.65	2.0/1.8	2.2/1.9	20/15
Hybrid 75225 (GLF23)	3.0/2.95	1.3/1.25	0.65/0.56	3.4/2.9	2.8/2.7	3.1/3.2	8.2/10
Hybrid 75225 (GLF23+CDBM)	2.6/2.95	1.15/1.25	0.57/0.56	2.8/2.9	2.2/2.7	3.2/3.2	10/10
Hybrid 48158 (GLF23)	2.0/2.6	1.05/1.07	0.35/0.50	1.40/1.55	1.8/2.0	3.4/2.5	5.0/6.0
Hybrid 48158 (GLF23+CDBM)	2.1/2.6	0.98/1.07	0.40/0.50	1.64/1.55	1.5/2.0	2.4/2.5	5.4/6.0
<i>rms</i>	15.6%	12.2%	17.1%	8.7%	17.6%	16.3%	18.2%

TABLE I Comparison between the simulations performed in this paper (left at each column) and the values obtained from experimental profiles (right at each column) for a number of global quantities. The rms for each quantity, representing the deviation over the set of simulation and models applied, is shown in the last row

Predictions for different JT-60SA scenarios have been carried out with CRONOS following the general results presented in the previous sections. Here only the flat-top stationary regime of the hybrid scenario is shown in figure 4. For this purpose, simulations including plasma current, heat and particle transport as well as pedestal have been performed. The general boundary conditions, in terms of magnetic and geometric quantities as well as the amount of heating power, have been obtained from previous 0-D simulations [1], scenario 4.2, and no further optimization or analysis has been carried out. GLF23 has been used for particle transport, and two simulations, one with GLF23 and another one with CDBM have been considered for heat transport. The pedestal width has been adjusted to follow the scaling $\Delta\psi_N = 0.076\beta_{p,ped}^{1/2}$ [10], where ψ_N is the normalized poloidal flux and $\beta_{p,ped}$ is the poloidal beta, $\beta_p = 2\mu_0 \langle P \rangle / B_p^2$, with B_p the poloidal magnetic field, calculated at the top of the pedestal. For this scenario, at $I_p=3.5\text{MA}$, input power 37MW and $B_t=2.2\text{T}$, $q_{95}\sim 4.5$ with $q < 1$ only for $\rho < 0.2$, and $H_{98}(y,2)\sim 1.2$ is obtained as shown in figure 4. The pedestal pressure is

Pped ~ 30 kPa located at $\rho=0.95$. The density profile is peaked, which is characteristic of this type of regime. The NBI fuelling is found to contribute little to this peaking.

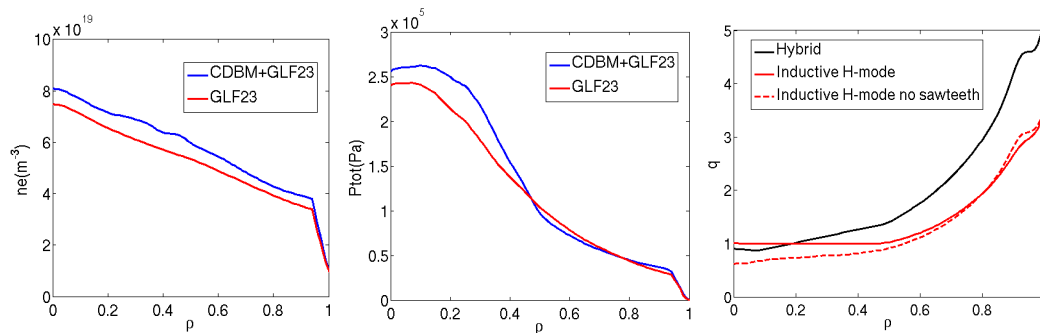


Figure 4 JT-60SA hybrid simulation densities (a) Total pressure (b) q profile (c) obtained with GLF23 and CDBM (only for heat transport)

Conclusions

An optimum set of models for the JT-60SA 1.5D scenario modelling has been obtained by analyzing core turbulence and pedestal MHD characteristics of selected discharges from JT-60U and JET, which share characteristics with JT-60SA. For inductive H-modes, heat and particle transport can be reasonably well simulated using the GLF23 transport model. The temperatures obtained are close to experimental data and the low density peaking, characteristic of these regimes is also recovered. However, for hybrid scenarios, the agreement between models and experimental data is less reliable. GLF23 tends to overestimate ion temperature. On the other hand, the CDBM transport model tends to give temperatures closer to experimental. Regarding particle transport, GLF23 is able to reproduce the increase of density peaking usually obtained in these regimes. Simulations including pedestal predictions together with particle and heat transport have been performed for JT-60U and JET inductive and hybrid discharges. The general rms is below 20% for the average densities and temperatures as well as for the pedestal pressure.

The analysis previously carried out gives a framework for JT-60SA modelling which has been used to simulate a hybrid scenario. In general, the typical characteristics of this type of scenario, high β_N and $H_{98}(y,2)$ have been recovered with the present design of machine subsystems on JT-60SA. This confirms, on the basis of the analysis of present day experiments, that the power and magnetic systems available on JT-60SA are adequate for the operation of these plasma scenarios defined in [1]. The simulation framework here analyzed is a good starting point for deeper analyses involving more sophisticated models for heat and particle transport.

This work was supported by EURATOM and carried out within the framework of the European Fusion Development Agreement. The views and opinions expressed herein do not necessarily reflect those of the European Commission.

References

- [1] JT-60SA Research Plan -Research Objectives and Strategy Version 3.0 2011, December, http://www.jt60sa.org/pdfs/JT-60SA_Res_Plan.pdf
- [2] Erba M. et al., Plasma Phys. Control. Fusion **39** 261 (1997).
- [3] Honda M. et al., Nucl. Fusion **46** 580 (2006).
- [4] Kinsey J.E. et al., Phys. Plasmas **12** 052503 (2005)
- [5] Artaud J.F. et al., Nucl. Fusion **50** 043001 (2010).
- [6] Hayashi N. et al., Phys. Plasmas **17** 056112 (2010).
- [7] Cordey J. G. Nucl. Fusion **43** 670-674 (2003).
- [8] Schneider M., Eriksson L.G., Basiuk V. and Imbeaux F. Plasma Phys. and Control. Fusion **47** 2087 (2005).
- [9] Tani K., et al., J. Phys. Soc. Jpn. **50**, 1726 (1981).
- [10] Snyder P.B. et al., Nucl. Fusion, **51** 103016 (2011).